ELSEVIER

Biochimica et Biophysica Acta 1440 (1999) 275–288

BIOCHIMICA ET BIOPHYSICA ACTA
BBA

www.elsevier.com/locate/bba

A structural comparison of the total polar lipids from the human archaea *Methanobrevibacter smithii* and *Methanosphaera stadtmanae* and its relevance to the adjuvant activities of their liposomes[1]

G. Dennis Sprott *, Jean-Robert Brisson, Chantal J. Dicaire, Anne K. Pelletier, Lise A. Deschatelets, Lakshmi Krishnan, Girishchandra B. Patel

Institute for Biological Sciences, National Research Council of Canada, Ottawa, Ont. K1A 0R6, Canada

Received 26 April 1999; received in revised form 20 July 1999; accepted 20 July 1999

Abstract

Mice were immunized with bovine serum albumin (BSA) entrapped within archaeosomes (i.e. liposomes) composed of the total polar lipids (TPL) from the two methanogenic archaea common to the human digestive tract. *Methanobrevibacter smithii* archaeosomes boosted serum anti-BSA antibody to titers comparable to those achieved with Freund's adjuvant, whereas *Methanosphaera stadtmanae* archaeosomes were relatively poor adjuvants. An explanation for this difference was sought by analysis of the polar lipid composition of each archaeobacterium. Fast atom bombardment mass spectrometry and NMR analyses of the purified lipids revealed a remarkable similarity in the ether lipid structures present in each TPL extract. However, the relative amounts of each lipid species varied dramatically. The phospholipid fraction in *M. stadtmanae* TPL was dominated by archaetidylinositol (50 mol% of TPL) and the glycolipid fraction by β-Glc*p*-(1,6)-β-Glc*p*-(1,1)-archaeol (36 mol%), whereas in *M. smithii* extracts, both caldarchaeol and archaeol lipids containing a phosphoserine head group were relatively abundant. Liposomes prepared from purified archaetidylinositol and from *M. stadtmanae* TPL supplemented with increasing amounts of phosphatidylserine elicited poor humoral responses to encapsulated BSA. A dramatic loss in the adjuvanticity of *M. smithii* archaeosomes was seen upon incorporation of 36 mol% of the uncharged lipid diglucosyl archaeol and, to a lesser extent, of 50 mol% of archaetidylinositol. Interestingly, the relative rates of uptake of *M. smithii* and *M. stadtmanae* archaeosomes by phagocytic cultures in vitro were similar. Thus, the lipid composition may influence archaeosome adjuvanticity, particularly a high diglucosyl archaeol and/or archaetidyl inositol content, resulting in a low adjuvant activity.

Keywords: Polar lipid structure; Archaeosome; Liposome; Adjuvant; Human archaea; *Methanobrevibacter smithii*; *Methanosphaera stadtmanae*

Abbreviations: BSA, bovine serum albumin; TPL, total polar lipids; A_S, standard archaeol, standard diether or 2,3-di-*O*-phytanyl-*sn*-glycerol; C_S, standard caldarchaeol, standard tetraether or 2,2′,3,3′-tetra-*O*-dibiphytanyl-*sn*-diglycerol; A_{OH}, hydroxyarchaeol; DGA_S, diglucosyl archaeol; PGP-O-CH_3, phosphatidylglycerol phosphate-*O*-methyl; GC/MS, gas chromatography/mass spectrometry; FAB, fast atom bombardment

* Corresponding author. Fax: +1 (613) 9411327; E-mail: dennis.sprott@nrc.ca

[1] Publication number 42395 of the National Research Council of Canada.

1388-1981/99/$ – see front matter
PII: S1388-1981(99)00130-4

1. Introduction

New adjuvants are required in vaccine formulations, partially because there are few adjuvants approved for human use and partially because molecular techniques have paved the way for the production of purified antigens having less unwanted side reactions, but less immunogenicity than crude preparations. Although alum is approved, it promotes primarily a Th2 response, which is non-protective against various intracellular pathogens [1]. A liposome-based vaccine against hepatitis A has been licensed for human use [2]. However, the relatively low 'immunomodulator' activity of this type of 'vehicle' adjuvant [3] has prompted a need to co-deliver additional adjuvants such as the lipid A or monophosphoryl lipid A components of endotoxins [4].

The interaction of lipid vesicles with tissue culture cells unexpectedly revealed that archaeosomes (liposomes prepared from polar archaeobacterial lipids) were taken up several fold better by phagocytic cells than conventional liposomes [5], implying more effective targeting to antigen presenting cells. In mouse trials, archaeosomes of several compositions were compared to several conventional liposomes and found to elicit much higher humoral responses to bovine serum albumin (BSA), an encapsulated soluble protein. The anti-BSA antibody titers in mouse sera were similar to those achieved with the potent, but toxic, Freund's adjuvant [6].

With regulatory issues in mind, we reasoned that it may be prudent to use the lipids from those archaeobacteria already inhabiting the human colon. Indeed, the methanogenic bacteria *Methanobrevibacter smithii* and *Methanosphaera stadtmanae* represent the only two archaeobacterial species found in humans and can approach $\geq 10^{10}$ cells per gram feces [7]. Here, we present the first comparison of the adjuvant/carrier properties of archaeosomes prepared from *M. smithii* and *M. stadtmanae* polar lipids and explain their contrasting adjuvant properties by elucidating the structures and relative abundance of their major lipids.

2. Materials and methods

2.1. Materials

Fatty acid free BSA, dipalmitoyl D,L-α-phosphatidyl-L-serine and Freund's adjuvants were purchased from Sigma Chemical (St. Louis, MO, USA). The LiposoFast system and 400 nm filters were from Avestin (Ottawa, Ont., Canada). Serum separator tubes were purchased from Becton Dickinson (Rutherford, NJ, USA) and horseradish peroxidase-conjugated goat anti-mouse IgG+IgM was from Caltag (South San Franscisco, CA, USA). EIA microtitration plates for ELISA reactions were sold by ICN Biomedicals (Aurora, OH, USA). [2-^{14}C]mevalonic acid and cholesteryl [1,2-^{3}H]hexadecyl ether were from NEN Life Sciences Products (Boston, MA, USA). Silica gel G-25 (0.25 mm), 20×20 cm glass plates were from Macherey-Nagel (Germany).

2.2. Archaeal strains and growth

M. smithii ALI (DSM 2375) and *M. stadtmanae* MCB-3 (DSM 3091), isolates from human feces, were obtained from the Deutsche Sammlung von Mikroorganismen und Zellkulturen (DSM). The growth media for the cultures were described by Choquet et al. [8], except that formate was omitted from the medium for *M. smithii*. Cultures were grown in a Chemap AG fermenter at 35°C in 55 l media as described previously [8]. Cells in the mid to late exponential growth phase were harvested and the cell paste was stored at −20°C prior to lipid extraction.

2.3. Lipid preparation and purification

Lipids were extracted from frozen-thawed cell pastes by the Bligh and Dyer method and a total polar lipids fraction (TPL) was obtained by precipitation with acetone, as described before [9]. TPL was separated into lipid bands by thin-layer chromatography (TLC) using silica gel G-25 and $CHCl_3$:CH_3OH:CH_3COOH:H_2O (85:22.5:10:4, v/v) for development. When plates were developed in a second dimension, the solvent was $CHCl_3$:CH_3OH:7 N NH_4OH (60:35:8, v/v). Lipid spots were located with iodine vapor and re-purified as necessary. Neg-

ative ion fast atom bombardment mass spectrometry (FAB MS) was used to assess purity and to determine the most probable identity of lipids recovered from the silica, based on the m/z of the respective molecular ions. Amino-positive lipids were detected on thin-layer plates with ninhydrin [10].

3-Hydroxyarchaetidylinositol ($A_{OH}PI$) and 3-hydroxyarchaetidylglycerol ($A_{OH}PG$) were purified from *Methanosarcina mazei* [11].

2.4. Preparation of archaeosomes

Archaeosomes were prepared aseptically by hydrating the TPL from *M. smithii* or *M. stadtmanae*, or the purified lipids, in sterile phosphate-buffered saline (PBS) (10 mM potassium phosphate, pH 7.14, 160 mM NaCl) containing 5 mg BSA/ml. Briefly, aliquots of 20 mg dry weight of lipids were dried in 25 ml glass vials, placed under vacuum for 1 h and hydrated in 1.0 ml PBS by shaking at 37°C for 24 h. Multilamellar archaeosomes, so formed, were converted by pressure extrusion through filters of a 400 nm pore size using a Liposofast (Avestin, Ottawa, Ont., Canada) to achieve a vesicle size range of about 200 ± 75 nm diameter, measured with a Nicomp 370 particle sizer in the vesicle mode, number-weighted (NICOMP, Santa Barbara, CA, USA). Any BSA not associated with the vesicles was removed by centrifuging at $200\,000 \times g_{max}$ for 30 min and washing the dispersed archaeosome pellet three times with 7 ml volumes of PBS. The amount of protein encapsulated per mg dry weight of proteoarchaeosomes was quantitated by sodium dodecyl sulfate (SDS)-Lowry following removal of lipid [12]. SDS-polyacrylamide gel electrophoresis of proteoarchaeosomes was performed to confirm the stability of the entrapped protein [6].

2.5. Inoculations

Female BALB/c mice at least 8 weeks of age were injected intraperitoneally at 0 and 14 days. When used, Freund's complete adjuvant was present in the first injection, incomplete in the second, both at 62.5% in PBS. Blood was collected from the tail veins, 7–16 days after the second immunization (as indicated in the figure legends). We have observed (L. Krishnan et al., unpublished) that maximal antibody titers are achieved within this time. The sera were titrated by a standard ELISA for anti-BSA antibody, as described previously [13].

2.6. Lipid distribution

Quantitation of polar lipid components in *M. smithii* and *M. stadtmanae* was done by labelling the lipids during growth in 100 ml aliquots of media containing 10 μCi of [2-^{14}C]mevalonic acid. Labelled total lipid extract was mixed with the respective unlabelled TPL and fractionated on triplicate silica G-25 plates by two-dimensional TLC ($CHCl_3$:CH_3OH:CH_3COOH:H_2O (85:22.5:10:4, v/v) in the first dimension and $CHCl_3$:CH_3OH:7 N NH_4OH (60:35:8, v/v) in the second. Lipid spots were visualized by viewing rhodamine-sprayed plates under ultraviolet light [10]. Each spot was removed with the adsorbent and counted in acidified aqueous counting scintillant. Negative ion MS of lipid spots was performed on a parallel plate loaded with the respective unlabelled lipid extract. Lipids were extracted from adsorbent corresponding to each spot prior to the analysis [14].

2.7. Head group analysis

Trifluoroacetic acid (TFA) or hydrofluoric acid (HF) hydrolyses were used to remove head groups for quantitation and identification by gas chromatography (GC)/MS as described [15] and by amino acid analysis. In some cases, hydrolysis by HF was used prior to TFA to identify the preferential release of phosphodiester-linked head groups from purified caldarchaeols. Dried lipids (0.25–0.5 mg) in plastic tubes were stored at 0°C for 12 h in 1.0 ml of 48% HF, dried under a N_2 stream and the HF-released head groups in the residue were dissolved in 2 ml CH_3OH plus 0.2 ml H_2O. The lipid moieties were removed by three 2 ml volumes of petroleum ether. The ether phases were combined, transferred to Reacti vials, dried under a stream of N_2 and hydrolyzed for 2 h at 100°C in 0.5 ml of 2 M TFA. TFA was removed with a N_2 stream and TFA-released head groups were dissolved in 0.5 ml H_2O. Both HF- and TFA-released head groups were acetylated by reduction with $NaBH_4$ (10 mg for 2 h at room temperature). Excess $NaBH_4$ was destroyed with acetic acid,

samples were dried by lyophilization and incubated at 100°C for 2 h in 0.5 ml acetic anhydride. The samples were taken to dryness under a stream of N_2 and dissolved in 1 ml $CHCl_3$ to which 1 ml H_2O was added. The $CHCl_3$ bottom phase was analyzed by capillary GC/MS.

2.8. NMR and MS

^{13}C NMR spectra were acquired at 300 K with a Bruker AMX-600 instrument operating at proton frequencies of 600 MHz. Purified lipids (4–5 mg) were dissolved in 0.8 ml d_6-benzene/d_4-methanol (7:1, v/v). Chemical shifts are reported relative to tetramethylsilane (0.0 ppm). Negative ion FAB MS spectra were recorded with a Jeol JMS-AX 505H instrument [11].

2.9. Phagocytosis assays

The J774A.1 monocyte cell line was maintained in RPMI 1640 medium (Gibco Life Technologies, NY, USA) supplemented with 8% fetal bovine serum (Hyclone Laboratories, UT, USA) at 37°C in a humidified 7% CO_2 incubator. Mouse peritoneal cells were obtained by peritoneal lavage from female BALB/c mice, 6–8 weeks of age. To obtain activated peritoneal macrophages, 1 ml of freshly prepared 3% thioglycollate (Difco) was injected intraperitoneally 4 days prior to peritoneal lavage. Archaeosomes for phagocytosis assays were prepared without BSA and labelled by including [^{3}H]hexadecyl cholesteryl ether with the polar lipids (10 μCi/mg lipids) prior to drying and hydration. For assessment of phagocytosis, J774A.1 or mouse peritoneal cells (10^5/well) were seeded overnight in 96 well microtiter tissue culture plates. In some cases, IFN-γ (1 ng/ml) was added to the cells to activate them. The next day, the cells were washed with PBS and incubated with archaeosomes (20–80 μg/well in a final volume of 0.2 ml) in RPMI 1640 medium supplemented with 8% FBS at 37°C. After 1–24 h incubations, the cells were washed with ice cold PBS containing 0.9 mM $CaCl_2$ to remove the non-adherent liposomes and then lysed with 0.5% n-octyl-β-D-glucopyranoside for 1 h at 37°C. The lysate was assessed for radioactive counts and protein by the BCA method (Pierce, IL, USA).

3. Results

3.1. Adjuvant properties of archaeosomes

In keeping with our previous findings [6], anti-BSA antibody titers in sera of mice receiving intraperitoneal injections of BSA encapsulated in *M. smithii* TPL archaeosomes were comparable to those achieved using Freund's adjuvant (Fig. 1). Central to this study was the observation that only comparably low titers of anti-BSA antibodies were found in sera of mice inoculated with BSA archaeosomes from *M. stadtmanae* TPL ($P < 0.01$ relative to titers for *M. smithii* archaeosomes). This difference in adjuvant activity could not be explained by size differences of the archaeosomes or by different loading efficiencies (Fig. 1). Furthermore, *M. stadtmanae* TPL archaeosomes failed to evoke a strong antibody response even in the long-term (beyond day 16, post-

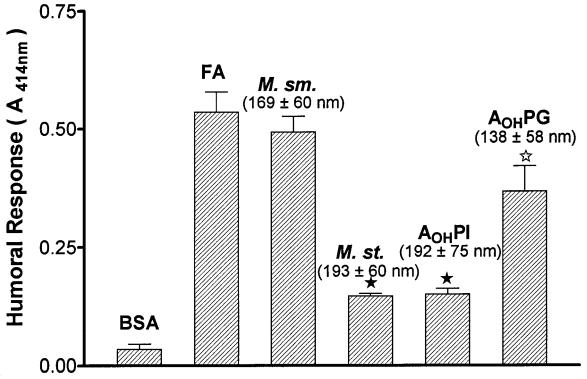

Fig. 1. Humoral response in BALB/c mice to BSA (12.5 μg/dose) encapsulated in archaeosomes. Intraperitoneal inoculations were on days 0 and 14 (three mice per group), blood was collected on day 21. The humoral response is shown as anti-BSA antibody (OD at 1:400 dilution) ± S.D.s measured by ELISA in mouse sera. BSA, no adjuvant/carrier; FA, Freund's adjuvant; *M. sm.*, BSA entrapped in *M. smithii* TPL archaeosomes (12.5 μg/1.2 mg lipids); *M. st.*, BSA entrapped in *M. stadtmanae* TPL archaeosomes (12.5 μg/1.1 mg lipids); $A_{OH}PI$, BSA entrapped in archaeosomes prepared from purified 3-hydroxyarchaetidylinositol (12.5 μg/0.34 mg lipid); $A_{OH}PG$, BSA entrapped in archaeosomes composed of purified 3-hydroxyarchaetidylglycerol (12.5 μg/0.37 mg lipid). Archaeosome diameters ± S.D.s are shown in the figure. Significantly reduced titers ($P < 0.01$ by Student's *t* test) for *M. stadtmanae* and $A_{OH}PI$ vesicles relative to *M. smithii* archaeosomes, ★. Titers for $A_{OH}PG$ are significantly enhanced ($P < 0.02$) relative to $A_{OH}PI$ liposomes, ☆.

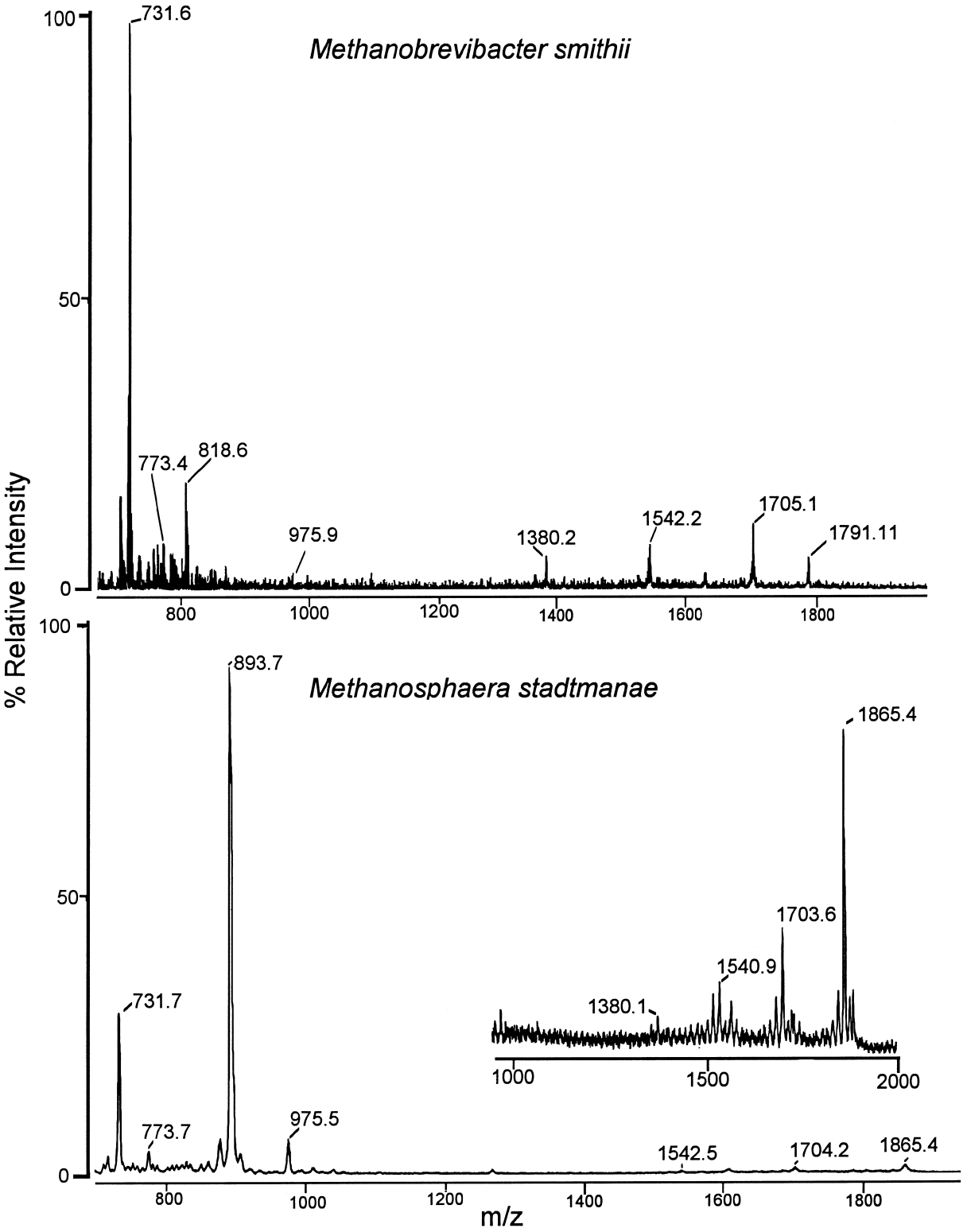

Fig. 2. Negative ion FAB MS analyses of TPL extracts from *M. smithii* (A) and *M. stadtmanae* (B). Frozen-thawed cell pastes were extracted with chloroform:methanol:water to obtain a total lipid extract. Neutral lipids were removed from the total lipids by precipitating the TPL with acetone. Negative ion FAB MS spectra are shown for each TPL.

immunization) and to other entrapped antigens (L. Krishnan et al., unpublished results), ruling out kinetic differences as a reason for the observed poor adjuvant activity. Clearly, detailed lipid structural information, currently lacking for the two genera of methanogens found in the human digestive tract, is required as a first step to understanding the mechanism(s) for the relative adjuvant properties of these archaeosomes. The importance of the choice of archaeal lipid used to construct the archaeosomes is illustrated further in Fig. 1. BSA archaeosomes prepared from purified 3-hydroxyarchaetidylinositol resulted in relatively low antibody titers ($P < 0.01$ relative to titers for *M. smithii* archaeosomes), whereas 3-hydroxyarchaetidylglycerol vesicles resulted in significantly higher titers ($P < 0.02$ relative to titers for archaetidylinositol).

3.2. FAB MS of TPL

Comparison of the negative ion FAB MS spectra of TPL from *M. smithii* and *M. stadtmanae* revealed a qualitative similarity in the polar lipids found (Fig. 2). Quantitatively, however, there were several major differences evident in the phospholipid profiles. A relatively dominant signal of m/z 731.6 arising from the summation of archaetidic acid (P-A_S) and the [P-A_S]$^-$ fragment typically formed from archaeol phospholipids was found in *M. smithii* lipid extracts. Also, signals corresponding in m/z to archaetidylserine (818.6) and diglucosyl caldarchaetidylserine (1791.1) were evident only in *M. smithii* TPL. Finally, signals expected for other caldarchaeol lipids (m/z 1705.1, 1542.2 and 1380.2) were more abundant in TPL from *M. smithii*, in keeping with the contents of caldarchaeol lipids reported to be 23 and 13 mol% of the ether lipids found in *M. smithii* and *M. stadtmanae*, respectively [16]. In contrast to the spectrum of *M. smithii* lipids, the most striking phospholipid signal from *M. stadtmanae* extracts was at m/z 893.7, indicative of a high content of archaetidylinositol.

Polar lipids present in minor, or trace, amounts were observed by partial purification of each TPL by TLC and removal of adsorbent in narrow bands from which the concentrated lipid components were extracted for MS analysis. The m/z for [M-H]$^-$ by negative ion FAB MS and the structures consistent with the theoretical m/z for the molecular ions are tabulated in Table 1. With a few exceptions (m/z 805, 899.5 and 1791), the same m/z of lipid signals were present in both TPL extracts. The trace nature of many of these lipids can be assessed by their absence

Table 1
Comparison of polar lipid m/z signals [M-H]$^-$ from *M. smithii* and *M. stadtmanae* lipid extracts based on negative ion FAB MS

Structure[a]	*M. stadtmanae*	*M. smithii*	Calculated [M-H]$^-$ m/z
A_S-P	731.7	731.6	731.6
A_S-PE	773.7	773.4	773.7
A_S-Glc	813.2	813.6	813.8
A_S-PS	818.4 (t)	818.6	818.7
A_S-PG	805.4 (t)	Not detected	805.7
A_S-PGP-0-CH_3[b]	899.5 (t)	Not detected	899
A_{OH}-PG	821.4 (t)	821.5 (t)	821.7
A_S-PI	893.7	893.2 (t)	893.7
A_{OH}-PI	909.4 (t)	909.4 (t)	909.7
A_S-$(Glc)_2$	975.5	975.9	975.8
C_S-P	1 380.1 (t)	1 380.2 (t)	1380.2
Glc-C_S-P	1 540.9 (t)	1 542.2	1 542.3
$(Glc)_2$-C_S-P	1 703.6 (t)	1 705.1	1 704.4
$(Glc)_2$-C_S-PS	Not detected	1 791.1	1 791.4
$(Glc)_2$-C_S-PI	1 865.4 (t)	1 866.7 (t)	1 866.4

[a]TPL extracts and partially purified sub-fractions therefrom were analyzed by negative ion FAB MS to provide an initial characterization of the lipids present. Structures consistent with the m/z signals for [M-H]$^-$ are shown in the first column. In some cases, more than one structure is consistent with the same [M-H]$^-$. Lipids present in small or trace amounts (t) were detected by negative ion FAB MS only after partial purification by TLC.

[b]The structure of a minor lipid of m/z 899.5 is tentatively shown as A_S-PGP-O-CH_3.

from spectra of unconcentrated TPL (Fig. 2). An exception is likely to be found for glycolipids which are detected by our FAB MS analysis with a low sensitivity relative to most phospholipids (m/z 813 and 975) and for phosphoserine lipids. In our hands, dimyristoyl phosphoglycerol was detected with a sensitivity 11.8-fold greater than dipalmitoyl phosphoserine (not shown). Hydroxyarchaeols of phosphoglycerol and phosphoinositol of m/z 821.7 and 909.7 [11] were observed, but the position of the hydroxy moiety on the alkyl chains was not assessed because of the low abundance of these lipids. Confirmation for the presence of phosphohydroxyarchaeols in fractions enriched for these lipids was obtained by observing the presence of a fragment ion at m/z 747.7, a m/z 16 larger than the phosphoarchaeol fragment ion [11].

3.3. Head groups in TPL

To determine the lipidic head groups present in TPL from *M. smithii* and *M. stadtmanae*, lipids were subjected to TFA or HF hydrolysis and the hydrophilic moieties were derivatized for GC/MS analysis. Glucose was the only reducing sugar detected. Inositol was also present. Serine was identified by amino acid analysis as the only amino acid present in TFA hydrolysates of TPL from both methanogens, with TPL from *M. smithii* containing approximately 3-fold more serine than was found in *M. stadtmanae* TPL.

3.4. Lipid cores

Following hydrolysis of TPL to remove head groups, the core lipid fraction separated upon TLC into two major components characteristic of archaeol and caldarchaeol and minor amounts of hydroxyarchaeol (not shown). The numbering of the carbon atoms of these major core lipids is shown in Fig. 3. ^{13}C NMR chemical shifts are shown for the alkyl chain carbons of the most abundant archaeol polar lipids (Table 2) to confirm the structures predicted by FAB MS. Chemical shifts for carbon atoms of the lipid alkyl chains compare closely to archaeol [17] and are compared directly to a polar lipid purified from *M. mazei* which has a 3-hydroxyarchaeol lipid moiety. Large chemical shifts of C-17 and C-3, and

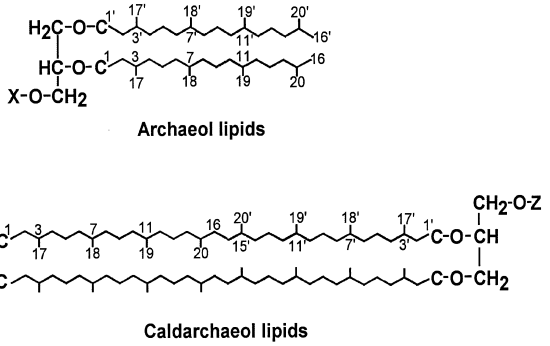

Fig. 3. Numbering of the chain regions of archaeol and caldarchaeol lipids found in *M. smithii* and *M. stadtmanae*. X, Y and Z are protons in the case of archaeol and caldarchaeol or other head group moieties in the case of the more polar lipids.

to a lesser extent C-2 and C-4, are caused by the 3-hydroxyl moiety [18]. By comparing to previous NMR data [17–19], it is seen that the chemical shifts fully support the assignment of the lipid chains of these archaeol lipids as 2,3-di-O-phytanyl-*sn*-glycerol. Similarly, the ^{13}C chemical shifts for the alkyl chain carbons of lipids of m/z 1866, 1542 and 1704 purified from *M. smithii* (not shown) were characteristic of the caldarchaeol lipid core [17,19]. Other details which confirm the lipid structures follow.

3.5. m/z 813

M. smithii and *M. stadtmanae* lipid extracts contained a m/z signal of 813 $[M\text{-}H]^-$, which was lost in part into the acetone soluble fraction, features characteristic for a monoglycosyl archaeol [20]. This lipid was purified from the total lipid extract of *M. smithii* as a yellow fraction which was eluted with $CHCl_3$ from a column of silica gel just following the elution of neutral lipids. The negative ion FAB MS spectrum in the polar lipid region showed a single signal of m/z 813.6, which corresponds to monoglycosyl archaeol of a theoretical m/z 813.8 for $[M\text{-}H]^-$. Because glucose was the only lipidic sugar found in TPL, we deduce the structure to be a monoglucosyl archaeol.

3.6. m/z 893

The FAB MS spectrum of a major lipid purified from *M. stadtmanae* TPL extracts yielded a single m/z signal of 893.1 and a fragment ion of m/z 731.7,

characteristic of an archaetidylinositol. ^{13}C NMR chemical shifts compare favorably to those of standard archaetidylinositol from *M. mazei* (Table 3). The upfield shift of the singlet from the C-1 of the glycerol backbone (1 g) of about 70 ppm for glycolipids to a doublet of about 66 ppm for phospholipids is as expected [20]. These findings, together with the identification by GC/MS of inositol as the head group released following hydrolysis with HF, confirm the structure as archaetidylinositol.

3.7. *m/z* 818

An amino-positive lipid, purified from *M. smithii* lipid extract, exhibited a R_f on TLC of 0.33 compared to 0.23 for dipalmitoyl phosphoserine. $[M-H]^-$ was 818.6 with a phosphoarchaeol fragment signal of 731.6, as expected for an archaetidlyserine [21]. The structure was confirmed by the ^{13}C NMR chemical shifts found for the lipid (Table 2) and head group (Table 3) moieties, which compare favorably to the serine signals of dipalmitoyl phosphoserine, found to be 173.83, 56.38 and 65.89 (doublet) ppm.

3.8. *m/z* 975

A major ninhydrin-negative glycolipid was purified to greater than 90% purity from *M. smithii* TPL and a comparable lipid was purified from *M. stadtmanae* TPL. $[M-H]^-$ signals of m/z 976.0 and 975.8, respectively, were found by FAB MS analysis and 7–8% contamination could be accounted for by the presence of monoglucosyl archaeol of m/z 813.8. ^{13}C NMR spectra acquired on both purified lipids indicated the identity of the sugar residues as an unsubstituted β-glucopyranoside linked to a second β-glu-

Table 2
^{13}C NMR chemical shifts (ppm) of the alkyl chain carbons of purified ether lipids in d_6-benzene/d_4-methanol (7:1)

Carbon[a]	$A_{OH}PI$ (*M. mazei*)	A_SPI (*M. stadtmanae*)	A_SPS (*M. smithii*)	DGA_S (*M. stadtmanae*)	DGA_S (*M. smithii*)
1	67.73	69.23	69.33	69.09	69.09
1′	70.35	70.43	70.48	70.41	70.42
2	40.87	37.78	37.52	37.68	37.70
2′	37.29	37.48	37.52	37.34	37.36
3	72.43	30.5 ± 0.08	30.6 ± 0.07	30.5 ± 0.05	30.5 ± 0.1
3′	30.46	30.5 ± 0.08	30.6 ± 0.07	30.5 ± 0.05	30.5 ± 0.1
4	43.38	37.1 ± 0.2	38.1 ± 0.2	38.1 ± 0.07	38.0 ± 0.2
4′	38.1 ± 0.3	38.1 ± 0.2	38.1 ± 0.2	38.1 ± 0.07	38.0 ± 0.2
5	22.24	25.1 ± 0.02	25.3 ± 0.1	25.1 ± 0.05	25.1 ± 0.01
5′	25.06	25.1 ± 0.02	25.3 ± 0.1	25.1 ± 0.05	25.1 ± 0.01
6,6′	38.1 ± 0.3	38.1 ± 0.2	38.1 ± 0.2	38.1 ± 0.1	37.0 ± 0.2
7,7′	33.3 ± 0.1	33.5 ± 0.1	33.5 ± 0.2	33.4 ± 0.05	33.4 ± 0.04
8,8′	38.1 ± 0.3	38.1 ± 0.2	38.1 ± 0.2	38.1 ± 0.1	37.0 ± 0.2
9,9′	25.0 ± 0.04	25.08	25.11	24.97	25.03
10,10′	38.1 ± 0.3	38.1 ± 0.2	38.1 ± 0.2	38.1 ± 0.1	38.0 ± 0.2
11,11′	33.3 ± 0.1	33.5 ± 0.1	33.5 ± 0.2	33.4 ± 0.05	33.4 ± 0.04
12,12′	38.1 ± 0.3	38.1 ± 0.2	38.1 ± 0.2	38.1 ± 0.1	38.0 ± 0.2
13,13′	25.3 ± 0.01	25.41	25.41	25.38	25.39
14,14′	39.8 ± 0.01	39.91	39.91	39.89	39.89
15,15′	28.3 ± 0.01	28.47	28.48	28.46	28.46
16,16′	22.8 ± 0.06	23.0 ± 0.05	23.0 ± 0.07	22.9 ± 0.05	23.0 ± 0.05
17	26.76	20.1 ± 0.1	20.1 ± 0.1	20.0 ± 0.05	20.0 ± 0.05
17′	19.9 ± 0.06	20.1 ± 0.1	20.1 ± 0.1	20.0 ± 0.05	20.0 ± 0.05
18,18′	19.9 ± 0.06	20.1 ± 0.1	20.1 ± 0.1	20.0 ± 0.05	20.0 ± 0.05
19,19′	19.9 ± 0.06	20.1 ± 0.1	20.1 ± 0.1	20.0 ± 0.05	20.0 ± 0.05
20,20′	22.8 ± 0.06	23.0 ± 0.05	23.0 ± 0.07	22.9 ± 0.05	23.0 ± 0.05

[a]Carbons 5, 9 and 9′ assignments are according to DeRosa and Gambacorta [19].

Table 3
^{13}C NMR chemical shifts (ppm) for the head groups of purified ether lipids in d_6-benzene/d_4-methanol (7:1)[a]

Moiety	Carbon	$A_{OH}PI$ (*M. mazei*)	A_SPI (*M. stadtmanae*)	A_SPS (*M. smithii*)	DGA_S (*M. stadtmanae*)	DGA_S (*M. smithii*)
First moiety (near lipid)	1	76.98	76.72	173.20	104.21	104.20
	2	71.81[1]	71.95[1]	56.32 (d)	74.25[1]	74.20[1]
	3	73.03	73.16	65.35 (d)	77.08[2]	77.01[2]
	4	72.25[1]	72.41[1]		70.17[3]	70.12[3]
	5	74.95	74.94		75.83	75.75
	6	72.41[1]	72.52[1]		69.09	69.09
Second moiety (terminal)	1′				104.47	104.45
	2′				74.30[1]	74.28[1]
	3′				77.08[2]	77.07[2]
	4′				70.64[3]	70.60[3]
	5′				76.94	76.92
	6′				62.15	62.08
Glycerol backbone	1g	65.98 (d)	66.06 (d)	65.83 (d)	69.96	70.00
	2g	79.11 (d)	78.91 (d)	78.79 (d)	78.67	78.67
	3g	71.49	71.62	71.89	71.39	71.46

[a]Chemical shifts are shown for the head group regions of the lipids analyzed in Table 2. Superscripts $^{1-3}$ indicate signals which may be interchanged, respectively.

copyranoside end group (Table 3). The ^{13}C chemical shifts compare closely to those reported for a β-Glc*p*-(1,6)-β-Glc*p*-(1,1)-archaeol lipid [20,22]. The β configuration of the glycosidic linkages were further confirmed by ^{1}H NMR, which revealed anomeric signals at 4.46 ppm ($J_{1,2}$ 8.0 ± 0.2 Hz) and 4.60 ppm ($J_{1,2}$ 7.8 ± 0.2 Hz) for the diglycosyl archaeol from *M. smithii* and 4.46 ppm ($J_{1,2}$ 8.0 ± 0.2 Hz) and 4.57 ppm ($J_{1,2}$ 7.8 ± 0.2 Hz) for the similar lipid from *M. stadtmanae*. Thus, the structures of these 975 m/z glycolipids are both β-Glc*p*-(1,6)-β-Glc*p*-(1,1)-archaeol, identical to those found in several archaeobacteria previously [20,22–24].

3.9. Caldarchaeols

From *M. smithii* TPL extracts, lipids were purified with m/z signals for $[M-H]^-$ of 1542.5, 1703.5 and 1866.9, proving that these signals found in lipid mixtures (Fig. 1) correspond to metabolites, rather than arising solely as fragmentation products formed during the FAB MS analysis of larger, related lipids.

In the case of the 1704 m/z lipid from *M. smithii*, sufficient purified material was available for chemical studies. Hydrolysis with HF released head groups identified by capillary GC/MS as glucose (85% of head groups recovered) and inositol (15%). The presence of this low concentration of inositol may be explained by contamination with a phosphoinositol lipid. Further hydrolysis of the HF-hydrolyzed lipid moiety with TFA released only glucose, which accounted for 85% of the total glucose recovered by both hydrolyses. Thus, together with the known m/z of the molecular ion, the lipid appears to consist of glucose:phosphate:caldarchaeol in a 2:1:1 molar ratio. A lipid was found from *M. stadtmanae* with the same m/z for the molecular ion and with the same R_f (Table 1).

The 1542 m/z lipid purified from *M. smithii* TPL released glucose (100%) upon hydrolysis with TFA and no inositol. This lipid appears then to consist of phosphate:glucose:caldarchaeol in an equal molar ratio and was not analyzed further. However, another lipid of identical m/z separated upon two-dimensional TLC (Table 4), suggesting the presence of the caldarchaetidylinositol previously reported as part of the lipid profiles of other methanogens [23,24].

A diglucosyl caldarchaetidylserine was deduced as the structure of an amino-positive lipid with $[M-H]^-$ of 1791.1 (Table 1).

In other archaea, caldarchaeol lipids of 1866 m/z have been reported which have diglucosyl and phosphoinositol head groups [23,24]. Hydrolysis with HF of a lipid with this same m/z, purified from *M. smi-*

thii, resulted in release of head groups identified by capillary GC/MS as primarily inositol (inositol:glc 17:3). A subsequent hydrolysis with TFA released primarily glucose (glc:inositol 47:3), supporting the assignment of the structure as a diglucosyl caldarchaetidylinositol.

3.10. Lipid quantitation

Quantitation was performed by separating labelled TPL spots by two-dimensional TLC. Spots were located following reaction with rhodamine by viewing under ultraviolet light. Unlabelled lipids were identified on a parallel plate by eluting the lipids from the adsorbent and performing negative ion FAB MS (Table 4). Lipid extracts of *M. stadtmanae* were dominated by archaetidylinositol accounting for 50 mol% of the TPL. By contrast, this lipid corresponded to less than 8 mol% of *M. smithii* TPL. A large amount of the TPL lipids of *M. smithii* appeared in a spot of m/z 818.0, corresponding to archaetidylserine (30 mol%), with much of the remaining label distributed among several caldarchaeol lipids, diglucosyl archaeol (DGA_S) and a lipid of m/z 731.5 with an R_f of 0.72 in acidic solvent indicative of archaetidic acid (P-D_S). The relatively higher amounts in *M. smithii* TPL correspond favorably to the relative signal heights observed by FAB MS (Fig. 2). Caldarchaeol lipids of m/z 1866, 1704 and 1542 account for about 40 mol% of the TPL of *M. smithii* and about 8 mol% in *M. stadtmanae*. Caldarchaeol lipids 1866 and 1704 with low R_f values are likely to be overestimated in this analysis, because of the presence of unidentified ninhydrin-positive components (most likely the m/z 1791 diglucosyl caldarchaetidylserine). In *M. smithii* TPL, two lipids separated with an identical m/z of 1704 and two of m/z 975. However, the structures of these minor lipids were not determined further. It is also interesting that a minor lipid of m/z 899.5 was present in TPL extracts of *M. stadtmanae*, which corresponds in m/z exactly to the phosphatidylglycerol phosphate-0-methyl (PGP-0-CH_3) characteristic of extreme halophiles [25].

Capillary GC analysis of TPL hydrolysates was confirmatory in showing a glucose:inositol ratio of 2.0 ± 0.84 ($n = 3$) for *M. stadtmanae* and 20.6 ± 4.7 ($n = 4$) for *M. smithii*.

Table 4
Quantitation of lipid spots following TLC of the [^{14}C]TPL from *M. stadtmanae* and *M. smithii*[a]

TPL source	R_{f1}	R_{f2}	[M-H]$^-$ m/z	Ninhydrin	Mol%
M. smithii					
	0.08	0.02	1 704.8/1 866	+	34 ± 2
	0.12	0.11	821.4	+	2 ± 0.3
	0.20	0.02	1704.8	−	3 ± 0.05
	0.22	0.15	893.0/1 541.8/975.5	−	8 ± 0.6
	0.34	0.28	818.0	+	30 ± 2
	0.49	0.28	1 541.8	−	3 ± 0.2
	0.49	0.54	975.5	−	12 ± 0.4
	0.72	0.20	731.5	−	8 ± 0.6
M. stadtmanae					
	0.04	0.03	1 866.5/1 704	+	8 ± 2
	0.05	0.09	899.5	−	2 ± 0.6
	0.14	0.07	821.5/909.4	−	2 ± 0.2
	0.19	0.02	821.5	−	1 ± 0.1
	0.22	0.18	893.0	−	50 ± 3
	0.53	0.43	975.5	−	36 ± 2
	0.75	0.16	731.5	−	1 ± 0.5

[a][^{14}C]TPL was prepared from archaea grown in the presence of the phytanyl chain precursor [^{14}C]mevalonic acid. [^{14}C]Lipids mixed with the respective unlabelled TPL were separated by two-dimensional TLC and quantitated by removing spots for scintillation counting. Lipids were recovered from spots obtained by running plates with the unlabelled TPL for negative ion FAB MS analysis. In cases where more than one [M-H]$^-$ signal was present in a spot, the signals are shown in order of greatest relative intensity. Quantitative data are shown as average mol% ± S.E.M. for triplicate plates.

3.11. Lipid composition and adjuvant properties

Because 86% of the TPL of *M. stadtmanae* was found to consist of archaetidylinositol and DGA_S, it may be expected that one, or both, of these lipids impart a negative feature to the adjuvant properties of *M. stadtmanae* TPL. This was tested by measuring the anti-BSA antibody titers in sera of mice inoculated with BSA encapsulated in archaeosomes composed of *M. smithii* TPL, to which sufficient purified archaetidylinositol or DGA_S was added to achieve the respective mol% found in *M. stadtmanae* TPL (Fig. 4). Compared to *M. smithii* TPL archaeosomes, those vesicles made with *M. smithii* TPL supplemented with additional DGA_S (to achieve 36 mol%) gave significantly lower anti-BSA antibody titers ($P < 0.01$). These lower titers were comparable quantitatively to the group of mice receiving BSA encapsulated in *M. stadtmanae* archaeosomes or to those composed of pure archaetidylinositol liposomes (Fig. 1). To a lesser extent, 50 mol% of archaetidylinositol, or a combination of both archaetidylinositol and DGA_S in *M. smithii* archaeosomes, also resulted in decreased anti-BSA antibody titers.

Dipalmitoyl phosphoserine incorporated at 5, 15 and 30 mol% into TPL archaeosomes of *M. stadtmanae* resulted in no elevation of anti-BSA antibody titers in sera of inoculated mice (not shown).

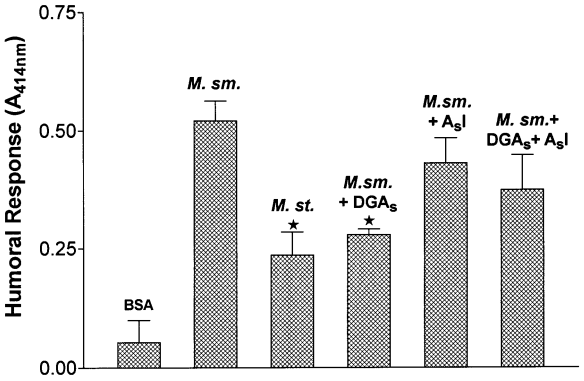

Fig. 4. Humoral response in BALB/c mice to BSA (10 μg/dose) encapsulated in archaeosomes prepared with *M. smithii* TPL supplemented with DGA_S and archaetidylinositol. BSA was encapsulated in archaeosomes of *M. stadtmanae* TPL or of *M. smithii* TPL ± purified DGA_S or archaetidylinositol added to achieve the mol% found in the TPL of *M. stadtmanae*. The lipid dose was maintained constant at 1.3 mg dry weight/injection by mixing with the respective empty archaeosomes prior to injection. The amount of BSA entrapped is shown below (in brackets) prior to dilution with empty archaeosomes. Intraperitoneal injections were given to mice in groups of four on days 0 and 14, blood was collected on day 31. BSA, no adjuvant/carrier; *M. sm.*, BSA encapsulated in *M. smithii* TPL archaeosomes (10 μg/ 0.65 mg lipids); *M. st.*, BSA encapsulated in *M. stadtmanae* TPL archaeosomes (10 μg/0.9 mg lipids); *M. sm.*+DGA_S, BSA encapsulated in *M. smithii* TPL+24 mol% DGA_S (10 μg/0.84 mg lipids); *M. sm.*+A_SI, BSA encapsulated in *M. smithii* TPL+42 mol% archaetidylinositol (10 μg/0.3 mg lipids); *M. sm.*+DGA_S+A_SI, BSA encapsulated in *M. smithii* TPL+24 mol% DGA_S+42 mol% archaetidylinositol. Archaeosome diameters in the order mentioned were 212 ± 76, 188 ± 65, 160 ± 69, 162 ± 67 and 258 ± 61 nm. The humoral response is shown as anti-BSA antibody in sera (OD at 1:400 dilution) ± S.D.s. Significantly reduced response for *M. st.* and *M. sm.*+DGA_S archaeosomes ($P < 0.01$, by Student's *t* test) relative to *M. sm.* TPL archaeosomes, ★.

3.12. Uptake by macrophages

Relatively different uptakes of the two archaeosome types into antigen presenting cells is one possible explanation for their contrasting adjuvant activities. Antigen presenting cells are commonly phagocytic. Therefore, the relative uptake of the two types of archaeosomes was compared in a monocyte/macrophage culture (J774A.1) and in a primary culture of mouse peritoneal macrophages. The relative extents of surface bound antigen on liposomes may influence opsonization and uptake by cells. However, both *M. smithii* as well as *M. stadtmanae* archaeosomes have similar amounts of surface bound BSA (< 20%, Krishnan, L. et al., unpublished results). This suggests that surface localization of antigen may have a similar influence on phagocytosis (if any) for both archaeosome types. Therefore, in order to address if differences in lipid composition per se influence uptake, we assessed phagocytosis of empty archaeosomes (without antigen). For J774A.1 cultures, a time course of uptake was established using 10, 20, 40 and 80 μg archaeosomes per well. Both *M. stadtmanae* and *M. smithii* archaeosomes were taken up in a linear, concentration dependent fashion over a 24 h period with the exception of the highest concentration of archaeosomes which saturated after about 6 h (not shown). Representative data for 40 μg/well revealed no significant difference in the rates of phagocytosis of either archaeosome type. Prior activation of J774A.1 cells by IFN-γ or peritoneal

macrophages with thioglycollate increased their overall phagocytic activity, but even under these conditions, both *M. smithii* and *M. stadtmanae* archaeosomes were phagocytosed to a similar extent (Table 5).

4. Discussion

Archaeosomes prepared from the TPL of the two genera of archaeobacteria commonly found in the digestive tract of humans exhibited contrasting adjuvant activities in mice. These effects could not be attributed to vesicle size, antigen loading and/or differences in kinetics of the humoral response. Further, there was no difference between the two pressure-extruded types of archaeosomes in the ratio of internalized:surface bound antigen (>4:1, Krishnan et al., unpublished results). Thus, we proceeded to characterize the polar lipids comprising each archaeosome to determine if there were substantial differences in lipid structure. Although the neutral lipids of *M. stadtmanae* have been analyzed [26], structural information is unavailable for the polar lipids of methanogens isolated from humans.

Both TPL extracts were initially characterized by negative ion FAB MS. The TPL of *M. stadtmanae* and *M. smithii* showed a remarkable similarity in the m/z of the molecular ions present (Table 1). Many of these lipids were found in only minor quantities, sometimes requiring enrichment for detection. Major lipids were purified and characterized by NMR methods as archaetidylinositol, archaetidylserine and β-Glc*p*-(1,6)-β-Glc*p*-(1,1)-archaeol. Indeed, glucose was the only hexose detected in lipid hydrolysates of both methanogens. These findings are consistent with, and extend, the report that inositol and serine form lipid head groups in *M. smithii* and inositol, serine and glucose in *M. stadtmanae* [27].

The lipid cores of *M. stadtmanae* are reported to consist of 79% archaeol, 13% caldarchaeol and 8% hydroxyarchaeol, whereas *M. smithii* TPL was found to contain higher amounts of caldarchaeol [9]. Indeed, the bulk of the polar lipid in *M. stadtmanae* was archaetidylinositol (50 mol%) and β-Glc*p*-(1,6)-β-Glc*p*-(1,1)-archaeol (36 mol%), reflecting an expected high content of archaeol.

In contrast, archaeols in *M. smithii* were dominated by archaetidylserine (30 mol%), lower contents of β-Glc*p*-(1,6)-β-Glc*p*-(1,1)-archaeol (12 mol%) and higher amounts of archaetidic acid (8 mol%). Morii et al. [24] reported several of the polar lipid structures in another species of *Methanobrevibacter*, *Methanobrevibacter arboriphilicus*, a methanogen isolated from the wet wood of a living tree. These were archaetidylserine (amount not determined), gentiobiosyl caldarchaetidylinositol (30%), gentiobiosyl caldarchaeol (9.9%), gentiobiosylarchaeol (12.6%), caldarchaetidylinositol (10.6%) and archaetidylinositol (3.1%). Although there are differences in the lipid structures found and in their relative abundance between the two strains of *Methanobrevibacter*, these are not great. Thus, the contrasting adjuvant activities observed between *M. smithii* and *M. stadtmanae* archaeosomes may be less dramatic in archaeosomes prepared from the TPL of strains within the same archaeal genus, where the lipid composition is more similar.

While the validity is uncertain in extrapolating results obtained with conventional ester lipids to archaeal lipids with similar head groups, it is clear that the lipidic head group can exert specific effects in vivo. Conventional liposomes composed of phosphatidylinositol are known to suppress both phagocyto-

Table 5
Comparison in uptake of *M. smithii* and *M. stadtmanae* archaeosomes by J774A.1 and mouse peritoneal macrophage cultures[a]

Culture	Activator	*M. smithii* archaeosomes		*M. stadtmanae* archaeosomes	
		6 h	24 h	6 h	24 h
J774A.1	None	48.8 ± 3.1	159.9 ± 19.8	41.1 ± 4.9	198.4 ± 27.9
J774A.1	IFN-γ	72.2 ± 21.9	226.8 ± 88.0	77.4 ± 27.5	288.1 ± 54.0
Peritoneal macrophages	Thioglycollate	125.3 ± 23.9	286.0 ± 66.2	126.0 ± 9.7	275.2 ± 56.8

[a]Phagocytosis assays were conducted by incubating adherent cells (30–40 μg protein/well) in 0.2 ml culture medium with 20–80 μg [^{3}H]archaeosomes. Representative data for 40 μg are shown in the table as μg archaeosomes taken up per mg culture protein.

sis and phospholipid metabolism in murine macrophages [28]. This finding may explain the relatively low adjuvant effect found for pure archaetidylinositol archaeosomes (Fig. 1). Also, phosphatidylserine is thought to be recognized by macrophages about to destroy apoptotic cells, by a mechanism involving CD36 [29]. Questions remain on the orientation of the lipids in the archaeosomes used herein. In membranes of *Methanobacterium thermoautotrophicum*, most β-Glc*p*-(1,6)-β-Glc*p* head groups were exposed to the outside of the cells, while serine and inositol residues oriented toward the cytoplasm [30]. Should this be the case in archaeosomes prepared from *M. stadtmanae* and *M. smithii* TPL, then, not only would the surface charge of each archaeosome type be different, but also much of the inositol and serine residues would remain unavailable for surface recognition by antigen presenting cells. Indeed, the phagocytosis by thioglycollate-activated murine peritoneal macrophages, or by J774A.1 cultures, of these two archaeosome types was not significantly different.

Major lipids were purified and incorporated into TPL archaeosomes during encapsulation of the antigen to evaluate their influence on the humoral response in mice. Because sufficient purified archaetidylserine was unavailable for this purpose, dipalmitoyl phosphoserine was substituted. Up to 30 mol% of this ester lipid was without benefit in increasing the adjuvanticity of *M. stadtmanae* archaeosomes, suggesting that the high adjuvanticity of *M. smithii* archaeosomes may not be explained solely by the high content of archaetidylserine. Certainly, archaetidylserine is apparently unnecessary for the comparably high adjuvant activities observed for several other archaeosome TPL compositions [6], such as those prepared from the TPL of *Thermoplasma acidophilum* which lacks archaetidylserine [31]. Adjuvant effects were not tested for all of the variables in lipid contents, notably, for the archaetidic acid and caldarchaeol lipids which were significantly higher in *M. smithii* TPL versus the TPL of *M. stadtmanae*. However, a striking decline in adjuvant activity was observed upon incorporation of 36 mol% of the uncharged lipid DGA_S, and to a lesser extent 50 mol% of archaetidylinositol, into TPL vesicles of *M. smithii* (Fig. 4). Archaeosomes composed of 100% archaetidylinositol were not particularly good adjuvants either (Fig. 1). Altered phagocytosis rates by antigen presenting cells seemed to be ruled out as an explanation for the contrasting adjuvant effects of various archaeosome compositions. However, other explanations could also be involved, such as differing mechanisms of adjuvant activity (through an immunomodulator versus a carrier effect), to variations in in vivo stabilities of various archaeosomes leading to altered antigen depot effects or to differences in antigen processing and presentation.

This study highlights the importance of the archaeal lipid composition in dictating the adjuvant activity of archaeosomes and shows that selection criteria should include low contents of DGA_S and archaetidylinositol. Further, the cost advantage anticipated in using a TPL extract, rather than attempting the challenging task of purifying specific archaeal lipids, may be realized by taking advantage of the strong adjuvant activity demonstrated for the TPL from the human methanogen *M. smithii*.

Acknowledgements

Mr. Perry Fleming is gratefully acknowledged for biomass production, Mr. Ken Chan for the FAB MS analyses and Miss Theresa Wiens for performing the initial phagocytosis assays.

References

[1] S.H.E. Kaufmann, Ann. Rev. Immunol. 11 (1993) 129–163.
[2] G. Gregoriadis, I. Gursel, M. Gursel, B. McCormack, J. Control. Release 41 (1996) 49–56.
[3] M. van Regenmortel, ASM News 63 (1997) 136–139.
[4] J.T. Ulrich and K.R. Myers, in: M.F. Powell and M.J. Newman (Eds.), Vaccine and Adjuvant Design: The Subunit and Adjuvant Approach. Plenum Press, New York, 1995.
[5] D.L. Tolson, R.K. Latta, G.B. Patel, G.D. Sprott, J. Liposome Res. 6 (1996) 755–776.
[6] G.D. Sprott, D.L. Tolson, G.B. Patel, FEMS Microbiol. Lett. 154 (1997) 17–22.
[7] T.L. Miller, M.J. Wolin, Syst. Appl. Microbiol. 7 (1986) 223–229.
[8] C.G. Choquet, G.B. Patel, T.J. Beveridge, G.D. Sprott, Appl. Microbiol. Biotechnol. 42 (1994) 375–384.
[9] G.D. Sprott, C.J. Dicaire, L.P. Fleming, G.B. Patel, Cells Mater. 6 (1996) 143–155.
[10] M. Kates, in: R.H. Burdon and P.H. van Knippenberg (Eds.), Techniques of Lipidology. Isolation, Analysis and Identification of Lipids. Elsevier, New York, 1986.

[11] G.D. Sprott, C.J. Dicaire, G.B. Patel, Can. J. Microbiol. 40 (1994) 837–843.
[12] D. Wessel, U.I. Flügge, Anal. Biochem. 138 (1984) 141–143.
[13] B. Makabi-Panzu, G.D. Sprott, G.B. Patel, Vaccine 15 (1998) 1504–1510.
[14] G.D. Sprott, C.G. Choquet and G.B. Patel, in: F.T. Robb (Ed.), Archaea: A Laboratory Manual. Cold Spring Harbour Laboratory Press, Cold Spring Harbour, NY, 1994.
[15] M.B. Perry, L. MacLean, D.W. Griffith, Biochem. Cell Biol. 64 (1986) 21–28.
[16] C.G. Choquet, G.B. Patel, G.D. Sprott, Can. J. Microbiol. 42 (1996) 183–186.
[17] I. Ekiel, I.C.P. Smith, G.D. Sprott, J. Bacteriol. 156 (1983) 316–326.
[18] G.D. Sprott, I. Ekiel, C.J. Dicaire, J. Biol. Chem. 265 (1990) 13735–13740.
[19] M. De Rosa, A. Gambacorta, Prog. Lipid Res. 27 (1988) 153–175.
[20] G. Ferrante, I. Ekiel, G.D. Sprott, J. Biol. Chem. 261 (1986) 17062–17066.
[21] H. Morii, M. Nishihara, M. Ohga, Y. Koga, J. Lipid Res. 27 (1986) 724–730.
[22] G. Ferrante, J.C. Richards, G.D. Sprott, Biochem. Cell Biol. 68 (1990) 274–283.
[23] M. Nishihara, H. Morii, Y. Koga, J. Biochem. 101 (1987) 1007–1015.
[24] H. Morii, M. Nishihara, Y. Koga, Agric. Biol. Chem. 52 (1988) 3149–3156.
[25] M. Kates, N. Moldoveanu, L.C. Stewart, Biochim. Biophys. Acta 1169 (1993) 46–53.
[26] W.J. Jones, G.U. Holzer, Syst. Appl. Microbiol. 14 (1991) 130–134.
[27] Y. Koga, M. Akagawa-Matsushita, M. Ohga, M. Nishihara, Syst. Appl. Microbiol. 16 (1993) 342–351.
[28] N.M. Wassef, F. Roerdink, E.C. Richardson, C.R. Alving, Proc. Natl. Acad. Sci. USA 81 (1984) 2655–2659.
[29] V.A. Fadok, M.L. Warner, D.L. Bratton, P.M. Henson, J. Immunol. 161 (1998) 6250–6257.
[30] M. Nishihara, Y. Koga, J. Biol. Chem. 269 (1994) 10492–10497.
[31] M. Swain, J.-R. Brisson, G.D. Sprott, F.P. Cooper, G.B. Patel, Biochim. Biophys. Acta 1345 (1997) 56–64.